

PRESSURE-BASED VENTING THERMAL MODEL FOR THE *DREAM CHASER*[®] SPACECRAFT CARGO SYSTEM

R. S. Miskovich
ATA Engineering, Inc.

S. W. Miller
Sierra Nevada Corporation

ABSTRACT

As a part of the design and testing of the Dream Chaser Cargo System, Sierra Nevada Corporation (SNC) wanted to simulate the venting and repressurization of the interstitial bays within the Dream Chaser Cargo System Thermal Desktop (TD) integrated thermal model (ITM). While venting may be simulated within TD's FloCAD module, SNC desired a stand-alone capability to perform venting simulations for various ascent and reentry conditions. Previously, SNC had a MATLAB simulation that took approximately 10 minutes to solve, and the team wanted a method that solved at a faster pace.

In response to this need, ATA Engineering (ATA) worked with SNC to develop a venting and repressurization software package called Venting and Repressurization (VRP) that can be used both as a stand-alone executable or coupled with TD. The software package assumes ideal gas properties, allowing the energy equations to be reformulated to solve directly for pressure and not temperature. The package was developed in Fortran to be compatible with TD's user-written subroutine capabilities. The package has been compared against equivalent TD FloCAD models and a version of the MATLAB code developed by SNC; it compares favorably to both. This paper will explore the software properties, strengths and benefits in modeling a Dream Chaser low-Earth orbit mission.

INTRODUCTION

SNC wanted to simulate the venting and repressurization of the Dream Chaser Cargo System unpressurized bays within its TD Dream Chaser Cargo System ITM. While venting can be simulated with TD's FloCAD module, FloCAD requires additional licenses, and SNC wanted to minimize the use of the FloCAD licenses. In addition, SNC desired a stand-alone capability to perform venting simulations for various different ascent and reentry conditions. Previously, SNC used a MATLAB simulation that took approximately 10 minutes to solve, and a faster method was preferred.

In response to this request, ATA developed a venting and repressurization software package called VRP that can be used as a stand-alone executable or coupled to TD. The package was developed in Fortran to be compatible with TD's user-written subroutine capabilities. The package has been compared against equivalent TD FloCAD models, as well as against a modified

version of the MATLAB code developed by SNC. An example comparison of the three codes is shown in Figure 1. The rest of this paper describes the different methods and codes that can be used to perform venting and repressurization simulations.

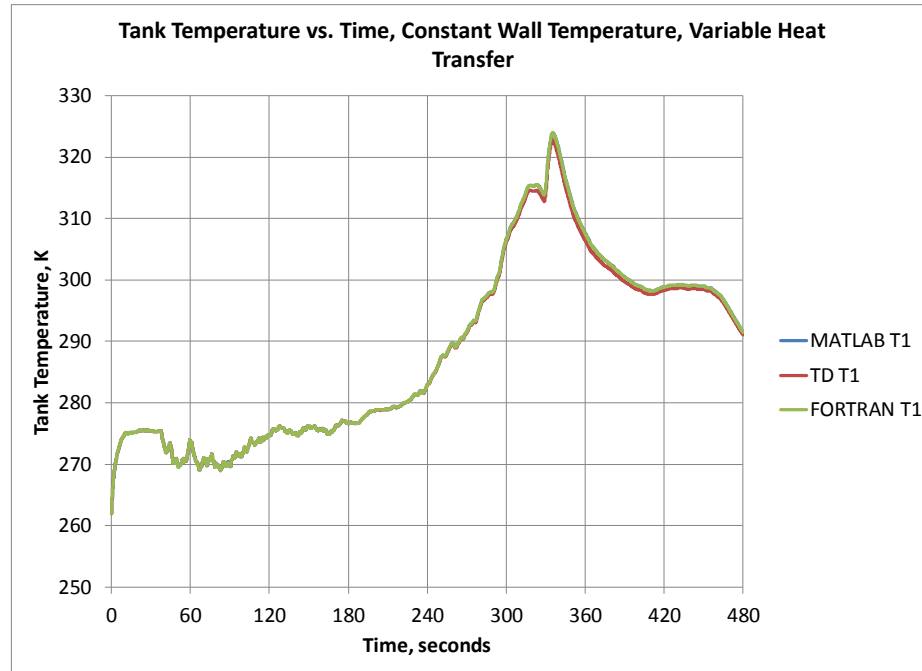


Figure 1. Example comparison for a repressurization simulation in MATLAB, TD, and Fortran program VRP.

VRP METHODOLOGY

The VRP methodology assumes that there are a series of compartments, or “tanks” in the VRP nomenclature, that are attached to other tanks through small orifices. There can be multiple orifices in and out of a tank. The velocity of air moving in a tank is low enough that it does not need to be included in energy or mass flow equations. Air is assumed to act as an ideal gas, and heat transfer to the walls of a tank is assumed to occur through natural convection instead of forced convection.

Conservation of Energy and Mass Equations for a Tank

The VRP code assumes that air will act as an ideal gas, with constant values for specific heat at constant pressure (C_p) and specific heat at constant volume (C_v). The equations of state for an ideal gas for a given pressure (P), temperature (T), universal gas constant (R), and density (ρ) or mass (M) are as follows:

$$P = \rho RT, \rho V = M \rightarrow PV = MRT$$

where internal energy (U) and enthalpy (H) are shown as

$$U = MC_vT$$

$$H = U + PV = MC_vT + MRT = MC_pT$$

and the specific heat ratio (γ) is

$$C_v + R = C_p$$

$$\gamma = \frac{C_p}{C_v}$$

The energy and mass transfer equations for a tank undergoing pressure change due to power (\dot{Q}) and mass flow in and out (Figure 2) are from Bird, Stewart, and Lightfoot [1]:

$$\frac{dH_{tank}}{dt} = \dot{Q}_{in} - \dot{Q}_{out} + V \frac{dP}{dt}$$

$$\frac{dM_{tank}}{dt} = \dot{m}_{in} - \dot{m}_{out}$$

where

$$\dot{Q}_{in} = \dot{m}_{in}C_pT_{in}$$

$$\dot{Q}_{out} = \dot{m}_{out}C_pT_{tank}$$

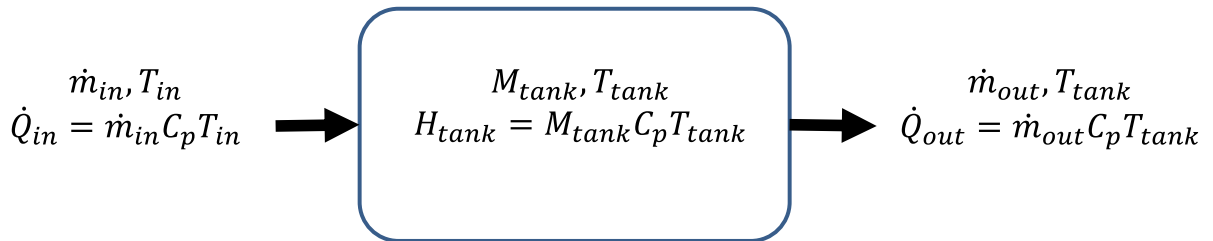


Figure 2. Schematic showing mass and energy transfer for a tank under venting or pressurization.

This equation can also be expressed as follows:

$$\frac{dH}{dt} = \frac{d(U + PV)}{dt} = \frac{dU}{dt} + P \frac{dV}{dt} + V \frac{dP}{dt} = \dot{Q}_{in} - \dot{Q}_{out} + V \frac{dP}{dt}$$

$$\frac{dU}{dt} = \dot{Q}_{in} - \dot{Q}_{out} - P \frac{dV}{dt}$$

Since the tank volume does not change:

$$\frac{dU}{dt} = \dot{Q}_{in} - \dot{Q}_{out}$$

This equation can be used to solve for the change in temperature:

$$\frac{d(M_{tank} C_v T_{tank})}{dt} = C_v T_{tank} \frac{dM_{tank}}{dt} + M_{tank} C_v \frac{dT_{tank}}{dt} = \dot{m}_{in} C_p T_{in} - \dot{m}_{out} C_p T_{tank}$$

$$(\dot{m}_{in} - \dot{m}_{out}) C_v T_{tank} + M_{tank} C_v \frac{dT_{tank}}{dt} = \dot{m}_{in} C_p T_{in} - \dot{m}_{out} C_p T_{tank}$$

$$(\dot{m}_{in} - \dot{m}_{out}) T_{tank} + M_{tank} \frac{dT_{tank}}{dt} = \dot{m}_{in} \gamma T_{in} - \dot{m}_{out} \gamma T_{tank}$$

$$M_{tank} \frac{dT_{tank}}{dt} = \dot{m}_{in} (\gamma T_{in} - T_{tank}) - \dot{m}_{out} (\gamma - 1) T_{tank}$$

The change in temperature versus time can now be expressed in inlet mass flow rate and temperature, mass and temperature of the tank, outlet mass flow rate, and γ . Since the change in mass is known and the volume remains constant, the updated density is known, and the updated pressure can be computed from the updated density and temperature using the ideal gas equation of state.

The problem with the energy equations in this form is that the heat transfer in the fluid is driven by pressure and not temperature and can lead to instabilities in the numerical solution. If the energy equations can be rewritten so that the heat transfer is pressure-based instead of being based on temperature, it will be possible to remove these instabilities in the numerical solution. A method to reformulate the energy equations is shown below.

For an ideal gas, the energy equation can be rewritten as follows:

$$\frac{dU}{dt} = \frac{d(M_{tank} C_v T_{tank})}{dt} = \frac{C_v}{R} \frac{d(M_{tank} R T_{tank})}{dt} = \frac{C_v}{R} \frac{d(P_{tank} V)}{dt} = \frac{V}{\gamma - 1} \frac{dP_{tank}}{dt}$$

The heat load into the tank can be rewritten as follows:

$$\begin{aligned} \dot{m}_{in} C_p T_{in} - \dot{m}_{out} C_p T_{tank} &= \dot{m}_{in} C_p \frac{P_{in}}{\rho_{in} R} - \dot{m}_{out} C_p \frac{P_{tank}}{\rho_{tank} R} \\ &= \dot{m}_{in} \frac{\gamma}{\gamma - 1} \frac{P_{in}}{\rho_{in}} - \dot{m}_{out} \frac{\gamma}{\gamma - 1} \frac{P_{tank}}{\rho_{tank}} \end{aligned}$$

Therefore, the tank energy equation can be rewritten in the form of pressures and densities as

$$V_{tank} \frac{dP_{tank}}{dt} = \gamma \dot{m}_{in} \frac{P_{in}}{\rho_{in}} - \gamma \dot{m}_{out} \frac{P_{tank}}{\rho_{tank}}$$

and the change in density of the tank is

$$\frac{d\rho_{tank}}{dt} = \frac{\dot{m}_{in} - \dot{m}_{out}}{V}$$

The equations above assume that $P_{in} > P_{tank} > P_{out}$ and that \dot{m}_{in} and \dot{m}_{out} are positive. To make the equations not dependent on these assumptions, these equations can alternatively be written as follows:

$$V_{tank} \frac{dP_{tank}}{dt} = \gamma \dot{m}_{in} \frac{P_{max,in}}{\rho_{max,in}} + \gamma \dot{m}_{out} \frac{P_{max,out}}{\rho_{max,out}}$$

$$\frac{d\rho_{tank}}{dt} = \frac{\dot{m}_{in} + \dot{m}_{out}}{V}$$

where

$$\dot{m}_{in} = \frac{P_{in} - P_{tank}}{|P_{in} - P_{tank}|} \dot{m}_{in,0}(P_{max,in}, \rho_{max,in}, P_{min,in})$$

$$P_{max,in} = \max(P_{in}, P_{tank})$$

$$P_{min,in} = \min(P_{in}, P_{tank})$$

and

$$\dot{m}_{out} = \frac{P_{out} - P_{tank}}{|P_{out} - P_{tank}|} \dot{m}_{out,0}(P_{max,out}, \rho_{max,out}, P_{min,out})$$

$$P_{max,out} = \max(P_{out}, P_{tank})$$

$$P_{min,out} = \min(P_{out}, P_{tank})$$

Now, $\dot{m}_{in,0}$ and $\dot{m}_{out,0}$ are positive by definition and are functions of the pressures and densities of the tank, inlets and outlets. However, \dot{m}_{in} and \dot{m}_{out} can be either positive or negative. By substituting \dot{m}_{in} and \dot{m}_{out} into the modified energy equation, the equation becomes

$$V_{tank} \frac{dP_{tank}}{dt} = \gamma \frac{P_{in} - P_{tank}}{|P_{in} - P_{tank}|} \dot{m}_{in,0} \frac{P_{max,in}}{\rho_{max,in}} + \gamma \frac{P_{out} - P_{tank}}{|P_{out} - P_{tank}|} \dot{m}_{out,0} \frac{P_{max,out}}{\rho_{max,out}}$$

$$V_{\text{tank}} \frac{dP_{\text{tank}}}{dt} = \frac{\gamma \dot{m}_{\text{in},0} P_{\text{max,in}}}{\rho_{\text{max,in}} |P_{\text{in}} - P_{\text{tank}}|} (P_{\text{in}} - P_{\text{tank}}) + \frac{\gamma \dot{m}_{\text{out},0} P_{\text{max,out}}}{\rho_{\text{max,out}} |P_{\text{out}} - P_{\text{tank}}|} (P_{\text{out}} - P_{\text{tank}})$$

We now have equations that are in a pressure-based form that can be solved numerically without instability.

The next step is to include heat exchange from the walls, including the surface area (A) of the walls. This changes the energy equation to

$$\frac{d(M_{\text{tank}} C_v T_{\text{tank}})}{dt} = \dot{m}_{\text{in}} C_p T_{\text{in}} - \dot{m}_{\text{out}} C_p T_{\text{tank}} + hA(T_{\text{wall}} - T_{\text{tank}})$$

or

$$M_{\text{tank}} \frac{dT_{\text{tank}}}{dt} = \dot{m}_{\text{in}} (\gamma T_{\text{in}} - T_{\text{tank}}) - \dot{m}_{\text{out}} (\gamma - 1) T_{\text{tank}} + \frac{hA}{C_v} (T_{\text{wall}} - T_{\text{tank}})$$

and in terms of pressure:

$$V_{\text{tank}} \frac{dP_{\text{tank}}}{dt} = \frac{\gamma \dot{m}_{\text{in},0} P_{\text{max,in}}}{\rho_{\text{max,in}} |P_{\text{in}} - P_{\text{tank}}|} (P_{\text{in}} - P_{\text{tank}}) + \frac{\gamma \dot{m}_{\text{out},0} P_{\text{max,out}}}{\rho_{\text{max,out}} |P_{\text{out}} - P_{\text{tank}}|} (P_{\text{out}} - P_{\text{tank}}) + (\gamma - 1) hA (T_{\text{wall}} - T_{\text{tank}})$$

The terms $\frac{\gamma \dot{m}_{\text{in},0} P_{\text{max,in}}}{\rho_{\text{max,in}} |P_{\text{in}} - P_{\text{tank}}|}$ and $\frac{\gamma \dot{m}_{\text{out},0} P_{\text{max,out}}}{\rho_{\text{max,out}} |P_{\text{out}} - P_{\text{tank}}|}$ can be described as “volumetric flow rates,” as these terms have units of volume per unit time and can be expressed as \dot{V}_{in} and \dot{V}_{out} . If $(P_{\text{in}} - P_{\text{tank}})$ or $(P_{\text{out}} - P_{\text{tank}})$ is zero, the value of \dot{V}_{in} or \dot{V}_{out} will be limited based on a minimum pressure difference. The term $(\gamma - 1) hA (T_{\text{wall}} - T_{\text{tank}})$ can be expressed as a heat load Q .

For a system of tanks and orifices, the energy equations can be written in matrix form as follows:

$$[V] \frac{d\vec{P}}{dt} + [\dot{V}] \vec{P} = \vec{Q}$$

where $[V]$ is a diagonal matrix that contains the volume of each tank, $[\dot{V}]$ is a matrix of the volumetric flow rates, and \vec{Q} is a vector of heat loads. For numerical integration, the equation can be rewritten as follows:

$$[V] \frac{\vec{P}_{n+1} - \vec{P}_n}{\Delta t} + [\dot{V}] \vec{P}_{n+1} = \vec{Q}_n$$

$$([V] + [\dot{V}] \Delta t) \vec{P}_{n+1} = \vec{Q}_n \Delta t + [V] \vec{P}_n$$

where n is the current time step and $n + 1$ is the next time step. This allows the pressure at time step $n + 1$ to be computed by the results from time step n and the updated $[\dot{V}]$ matrix.

Finally, for heat transfer between the wall and the tank, the energy equation is

$$M_{wall}C_{p,wall}\frac{dT_{wall}}{dt} + hA(T_{wall} - T_{tank}) = 0$$

For numerical integration, this equation can be rewritten as follows:

$$M_{wall}C_{p,wall}\frac{T_{wall,n+1} - T_{wall,n}}{\Delta t} + hA(T_{wall,n} - T_{tank,n}) = 0$$

$$T_{wall,n+1} = T_{wall,n} - \frac{hA\Delta t(T_{wall,n} - T_{tank,n})}{M_{wall}C_{p,wall}}$$

Mass Flow Equations

The mass flow rate calculations are from Bird, Stewart, and Lightfoot [1] and are based on the upstream (P_1) and downstream (P_2) pressures where $P_1 > P_2$, the upstream density (ρ_1), the area of the orifice (A), the coefficient of discharge (C_d), γ , and whether the flow is choked. The flow is choked if

$$\frac{P_2}{P_1} < \left(\frac{2}{\gamma + 1}\right)^{\frac{\gamma}{\gamma - 1}}$$

and the flow rate is

$$\dot{m}(P_1, \rho_1, P_2) = C_d A \sqrt{\gamma P_1 \rho_1 \left(\frac{2}{\gamma + 1}\right)^{\frac{\gamma + 1}{\gamma - 1}}}$$

If the flow is not choked, then the flow rate is

$$\dot{m}(P_1, \rho_1, P_2) = C_d A \sqrt{2P_1 \rho_1 \left(\frac{\gamma}{\gamma - 1}\right) \left[\left(\frac{P_2}{P_1}\right)^{\frac{2}{\gamma}} - \left(\frac{P_2}{P_1}\right)^{\frac{(\gamma + 1)}{\gamma}} \right]}$$

Heat Transfer Equations between Tank Wall and Air

The heat transfer coefficient is based on natural convection of an enclosed sphere [2]. There are two different correlations of Nusselt number based on diameter (Nu_D) to Rayleigh number based on diameter (Ra_D):

$$Nu_D = 0.59(Ra_D)^{1/4}$$

and

$$Nu_D = 0.13(Ra_D)^{1/3}$$

To be consistent with TD's solver SINDA/FLUINT [3], the transition Rayleigh number is

$$Ra_{D,trans} = \left(\frac{0.59}{0.13}\right)^{12} \approx 7.64E7$$

TD EXAMPLE MODELS

Two TD models were created to validate the VRP code. Both models use an ideal gas air model with temperature-dependent conductivity and viscosity that are consistent with VRP and the modified MATLAB code. This section describes one of the TD models (the half model) used to validate the VRP code.

Half Model

The half model, shown in Figure 3, consists of 12 TD lumps that represent the unpressurized sections of the Dream Chaser Cargo System and one boundary condition. These lumps are connected by 12 orifices. This model is based on data used in the MATLAB model.

This model was used for four simulations. The first assumed adiabatic walls and therefore did not need any couplings to thermal nodes. The second simulation assumed a fixed wall temperature with a fixed heat transfer coefficient of 5 W/m²/K. A sink node with a temperature of 273 K was connected to each of the lumps by a tie, as shown in Figure 4. For lump one, the wall surface area was modeled as 3 m²; for lump two, it was 4 m²; and for the remaining lumps, it was 5 m². The third and fourth simulations used a variable heat transfer coefficient to a thermal node based on free convection in a sphere. For these cases, each lump was attached to its own thermal node, as shown in Figure 5. Each node was given a thermal capacitance equal to the surface area (again, 3 m² for lump one, 4 m² for lump two, and 5 m² for the remaining lumps) times a wall thickness of 0.125 inches times the density of aluminum (2700 kg/m³) times the specific heat of aluminum (960 J/kg/K). For the third simulation, the temperature of each one of these nodes was held at 273 K, and for the fourth simulation, the initial temperature was 273 K.

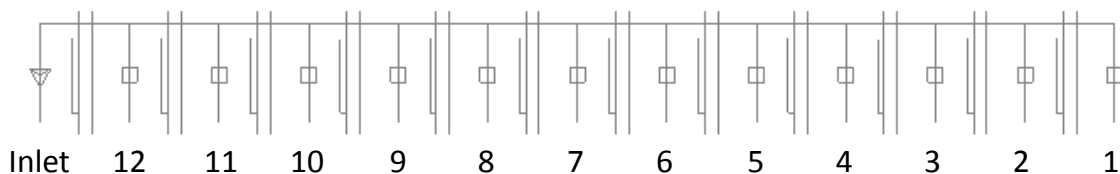


Figure 3. TD half model used for validation, showing lump IDs.

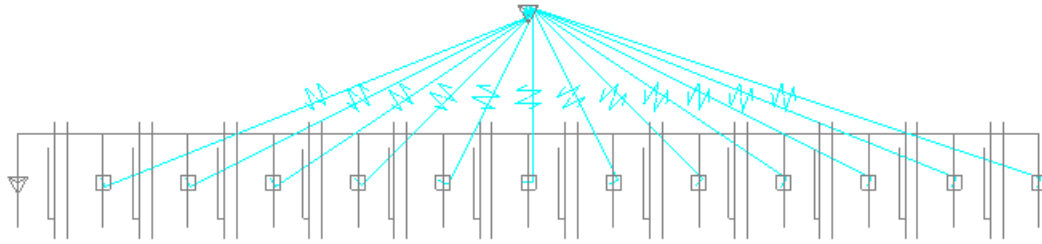


Figure 4. TD half model used for validation, showing tie connections to a single thermal node.

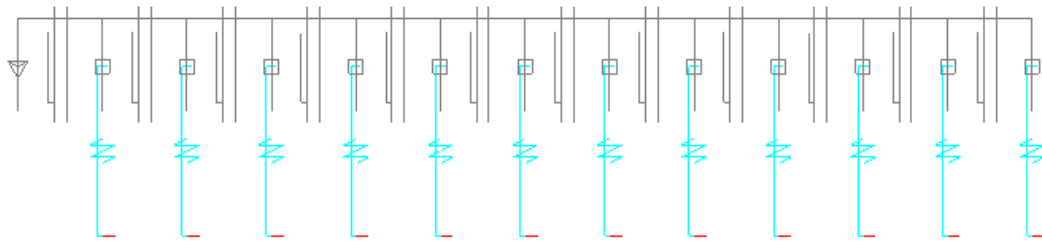


Figure 5. TD half model used for validation, showing tie connections between each lump and a corresponding thermal node.

COMPARISON OF MATLAB, TD, AND VRP STAND-ALONE

Four simulations were performed to validate the VRP code. These simulations used the half model and included results from MATLAB, TD and VRP. Each of the simulations used the same initial starting conditions and the same pressure profile. The only differences were whether there was heat transfer to a wall, how the heat transfer coefficient was computed and whether the wall temperature was fixed or was affected by heat transfer from the air to the wall.

Half Model, Adiabatic Wall

The first simulation used an adiabatic wall boundary condition. In this case, the enthalpy from the incoming air is used to heat up only the air in each of the compartments. The TD results for all compartments are shown in Figure 6, and a comparison of the three methods is shown in Figure 7. It is notable that the temperature for the first compartment exceeds 690 K with these conditions, and the three methods produce similar results.

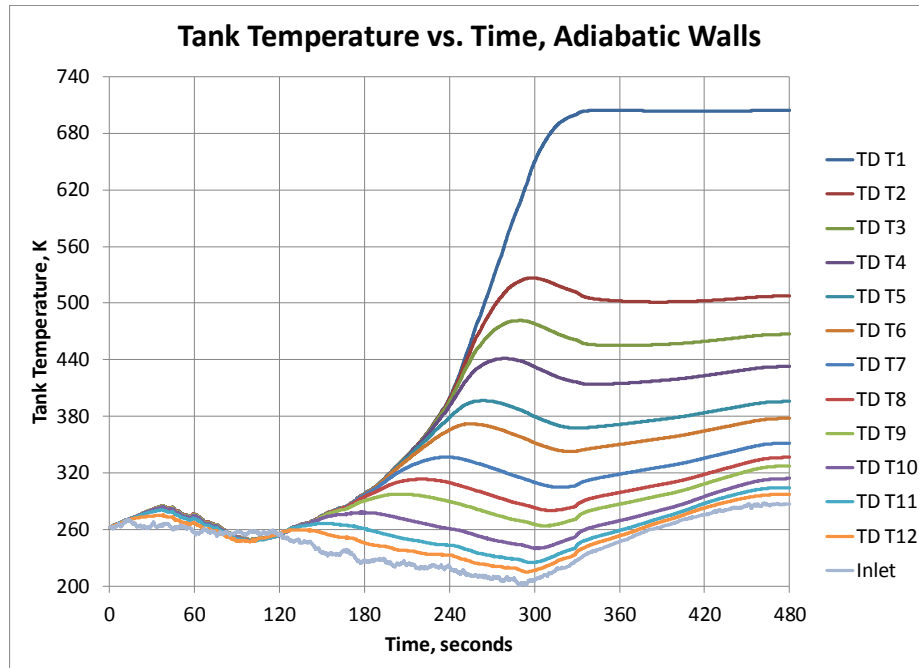


Figure 6. TD adiabatic repressurization temperatures.

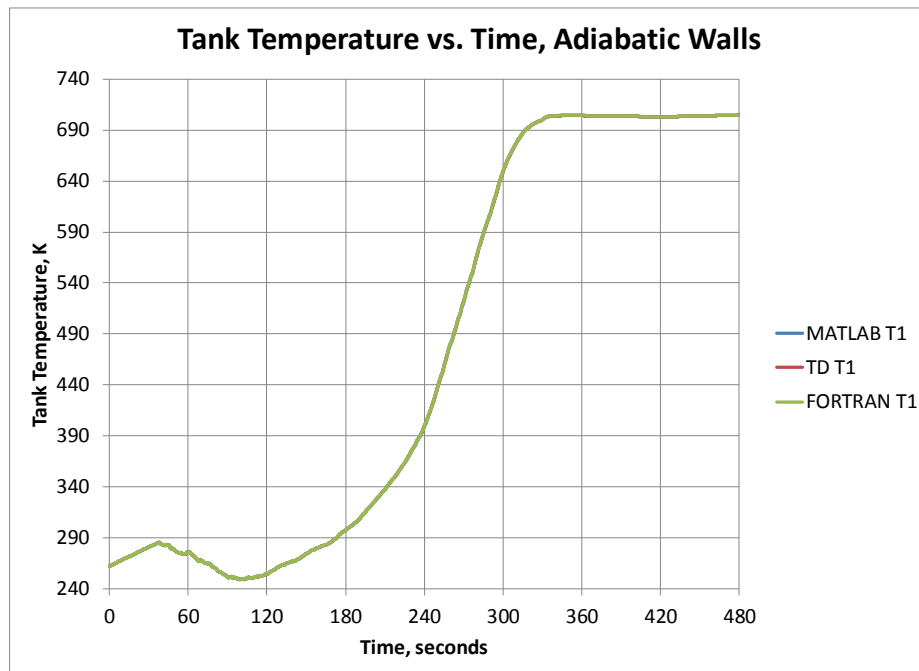


Figure 7. Air volume 1 comparison for adiabatic repressurization simulation in MATLAB, TD, and VRP.

Half Model, Constant Wall Temperature, Constant Heat Transfer

The second simulation used a constant heat transfer coefficient of $5 \text{ W/m}^2/\text{K}$ (a typical heat transfer coefficient value for natural convection at atmospheric pressure) to a fixed wall temperature of 273 K . The TD results for all compartments are shown in Figure 8, and a comparison of the three methods is shown in Figure 9. The air in the compartments stays at the wall temperature for nearly 200 seconds as the enthalpy of the incoming air is transferred to the wall sink temperature. Only after 200 seconds is the mass flow rate sufficient to cause a rise in the air volume temperatures, but the temperatures only rise to less than 300 K , showing that the wall can significantly affect the air compartment temperatures. The three methods again produce similar results.

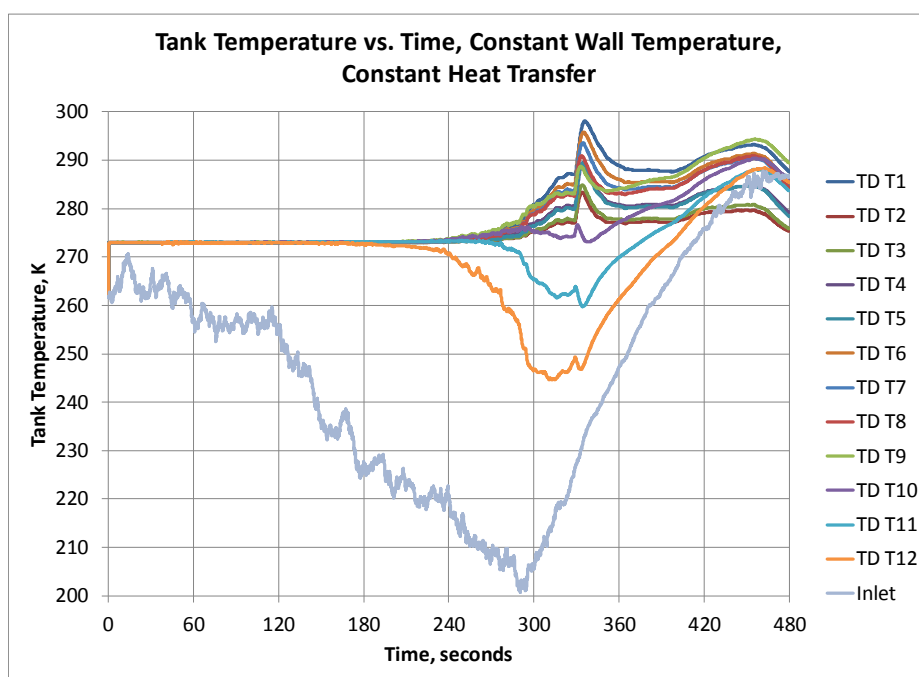


Figure 8. TD fixed heat transfer coefficient repressurization temperatures.

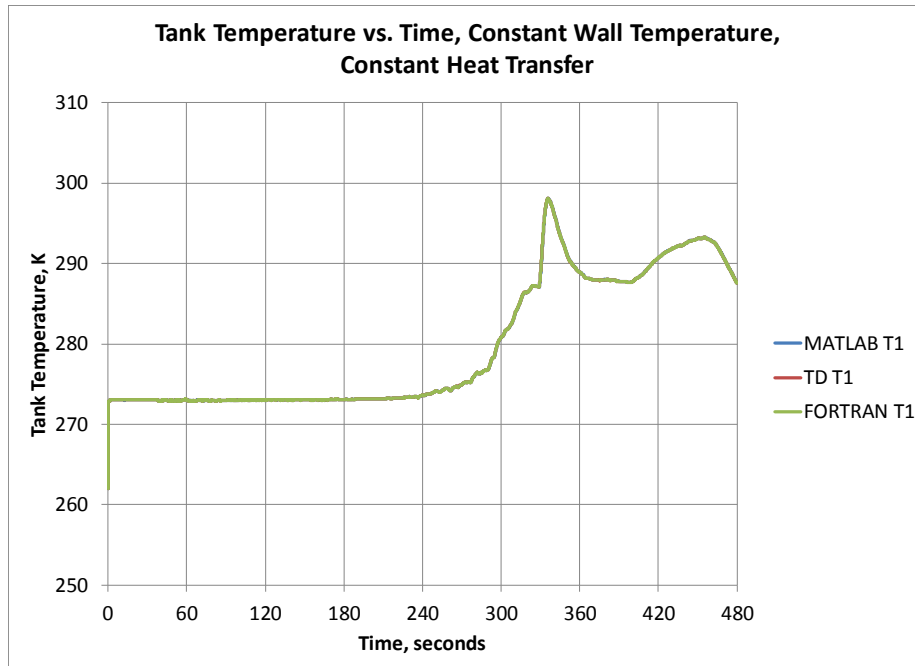


Figure 9. Air volume 1 comparison for fixed heat transfer coefficient repressurization simulation in MATLAB, TD and VRP.

Half Model, Constant Wall Temperature, Variable Heat Transfer

The third simulation used a variable natural convection heat transfer coefficient, which is dependent on compartment pressure, density, temperature and acceleration, to a fixed wall temperature of 273 K. The TD results for all compartments are shown in Figure 10, and a comparison of the three methods is shown in Figure 11. Unlike the previous case, the compartment air temperatures vary from the sink temperature in the first 200 seconds, as the heat transfer coefficient during this time is much lower than the fixed value of the previous simulation. Again, after 200 seconds, the air volume temperatures begin to rise, peaking at slightly over 320 K. Finally, with natural convection, there is a slight difference in the temperatures predicted by TD compared with MATLAB and VRP, but the difference is less than 2 K (Figure 11) and may be due to slight variations in the natural convection correlations as implemented in the three methods. The results are similar enough that the overall differences when used in the Dream Chaser Cargo System thermal model should be insignificant.

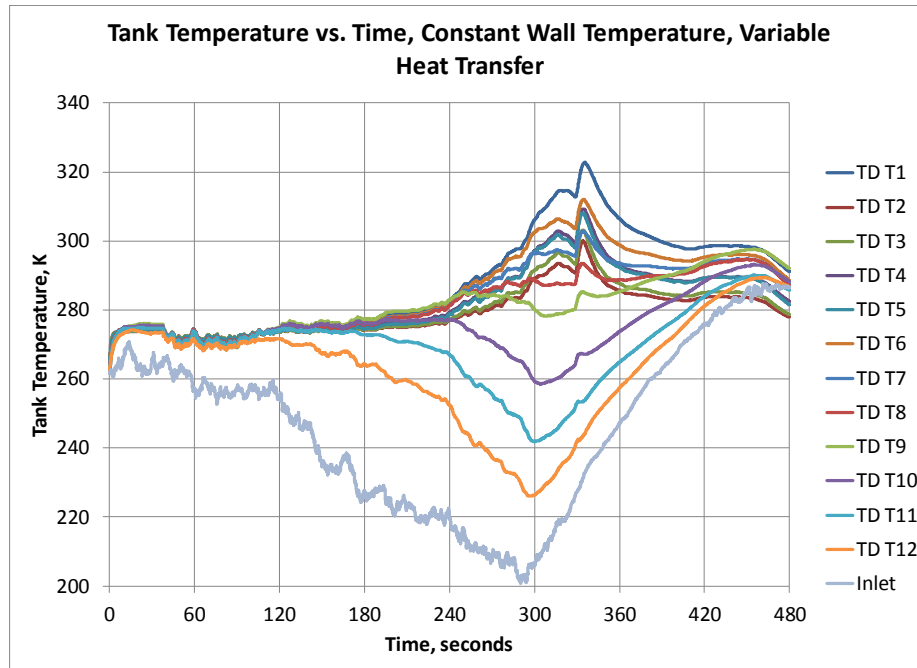


Figure 10. TD natural convection heat transfer coefficient repressurization temperatures.

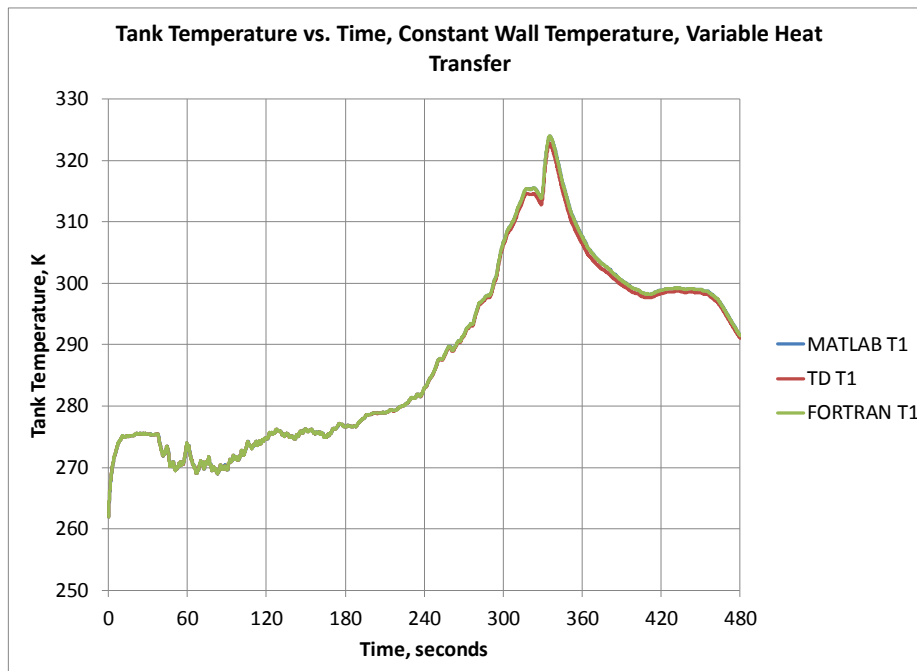


Figure 11. Air volume 1 comparison for natural convection heat transfer coefficient repressurization simulation in MATLAB, TD and VRP.

Half Model, Variable Wall Temperature, Variable Heat Transfer

The fourth simulation used a variable natural convection heat transfer coefficient, which is dependent on compartment pressure, density, temperature and acceleration, with each air compartment connected to a wall node with an initial temperature of 273 K and a thermal mass. The wall temperatures were modeled to change due to the heat gain or loss from the air. The TD results for all compartments are shown in Figure 12, and a comparison of the three methods is shown in Figure 13. The results for this simulation are similar to the previous simulation, as the wall temperatures did not vary significantly during the simulation, which is shown in Figure 14. This indicates that modeling the walls at a fixed temperature is a reasonable approximation. There is also a similar variation of the temperatures predicted by TD compared by MATLAB and VRP, but the difference is less than 2 K (Figure 13). It is important to model each bay explicitly and not to model multiple bays as a combined single bay.

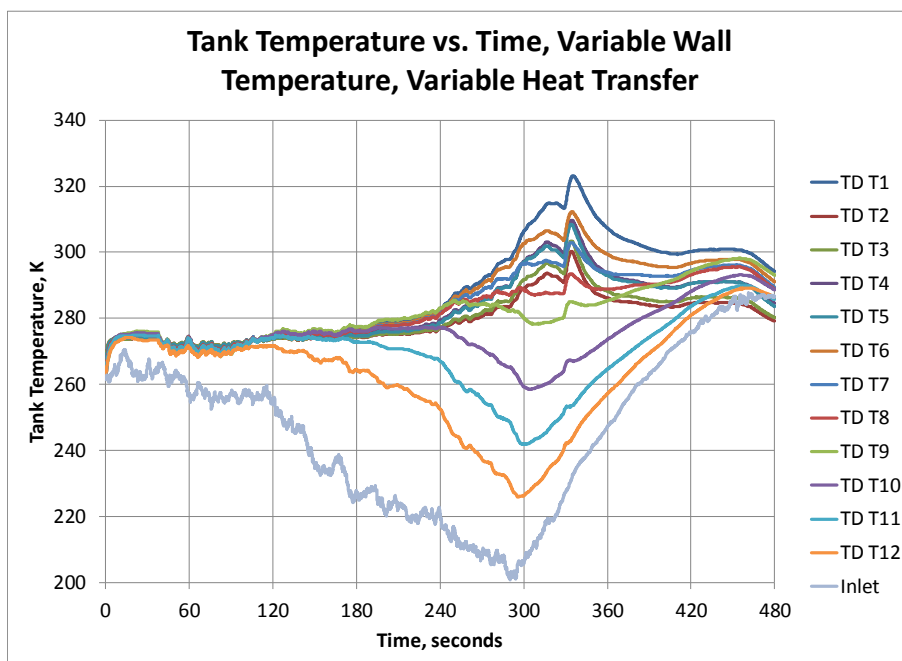


Figure 12. TD natural convection heat transfer coefficient with variable wall temperature repressurization temperatures.

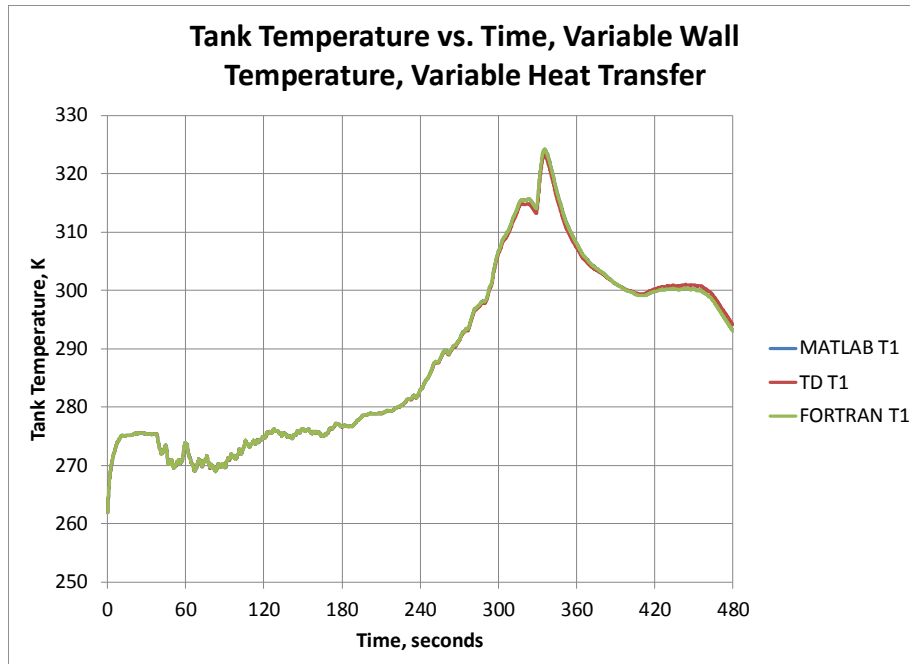


Figure 13. Air volume 1 comparison for natural convection heat transfer coefficient with variable wall temperature repressurization simulation in MATLAB, TD and VRP.

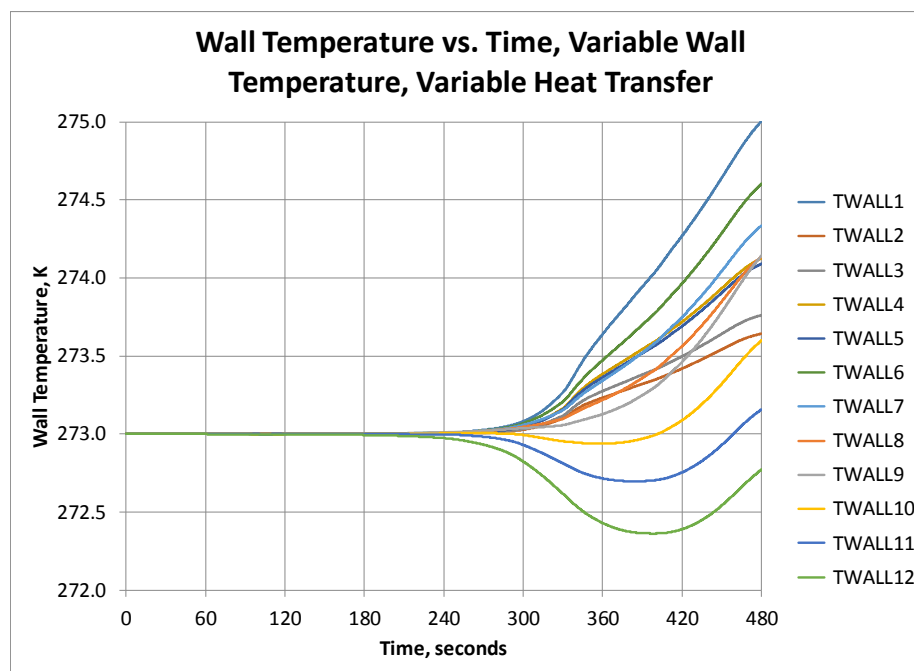


Figure 14. Wall temperatures for natural convection heat transfer coefficient with variable wall temperature repressurization simulation in VRP.

CONCLUSIONS

The VRP code successfully matches predictions from two independently developed methods using MATLAB and FloCAD. The code assumes that air acts as an ideal gas and that heat transfer from the air is applied via natural convection within a sphere. VRP has been integrated into the Dream Chaser Cargo System ITM using Fortran subroutine codes. When enabled, the code incorporates the effects of venting or repressurization on internal structure and components.

CONTACT

R. Scott Miskovich is currently a Senior Technical Advisor and Technical Director, Thermal, at ATA Engineering, Inc., and has been involved in thermal and fluid analysis for over 25 years at ATA Engineering and SDRC. He has a Master of Science degree in Mechanical Engineering and a Bachelor of Science in Engineering and Applied Science, both from the California Institute of Technology. He can be contacted at scott.miskovich@ata-e.com.

Stephen Miller is currently a Principal Systems Engineer at Sierra Nevada Corporation and the lead for the Dream Chaser Thermal Analysis Team. He has a Master of Science degree in Mechanical Engineering from the University of Houston and a Bachelor of Science in Mechanical Engineering from Texas A&M University. He can be contacted at stephen.miller@sncorp.com.

NOMENCLATURE, ACRONYMS, ABBREVIATIONS

γ	specific heat ratio
ρ	density
A	area
C_p	specific heat at constant pressure
C_v	specific heat at constant volume
H	enthalpy
ITM	Integrated thermal model
J	Joule
K	Kelvin
kg	kilograms
M	mass
\dot{m}	mass flow rate

m	meters
Nu	Nusselt number
P	pressure
\dot{Q}	power
R	universal gas constant
Ra	Rayleigh number
SNC	Sierra Nevada Corporation
T	temperature
TD	Thermal Desktop
t	time
U	internal energy
V	volume
VRP	Venting and Repressurization code
W	Watts

REFERENCES

1. Bird, R.B., W.E. Stewart, and E.N. Lightfoot. *Transport Phenomena*. John Wiley & Sons. 1960.
2. Guyer, E.C. *Handbook of Applied Thermal Design*. Taylor & Francis. 1999.
3. Cullimore, B.A., S.G. Ring, and D.A. Johnson, *SINDA/FLUINT User's Manual*, Version 5.8, C&R Technologies, Inc., June 2015.